17th International Conference on the Application of Computer
Science and Mathematics in Architecture and Civil Engineering
K. Gürlebeck and C. Könke (eds.)
Weimar, Germany, 12–14 July 2006

LIFETIME-ORIENTED OPTIMIZATION OF BRIDGE TIE RODS EXPOSED TO VORTEX-INDUCED ACROSS-WIND VIBRATIONS

M. Gálffy*, M. Baitsch, A. Wellmann Jelic and D. Hartmann

Institute of Computational Engineering, Faculty of Civil Engineering,
Ruhr-University Bochum
Universitätsstr. 150, D–44780 Bochum, Germany
*E-mail: mozes.galffy@rub.de

Keywords: Lifetime-oriented optimization, Notch stress approach, Stochastics, Wind induced excitations, Woehler-curves.

Abstract. *In recent years, damages in welded connections plates of vertical tie rods of several arched steel bridges have been reported. These damages are due to fatigue caused by wind-induced vibrations. In the present study, such phenomena are examined and the corresponding lifetime of a reference bridge in Münster-Hiltrup, Germany, is estimated, based on the actual shape of the connection plate. Also, the results obtained are compared to the expected lifetime of a connection plate, whose geometry has been optimized separately. The structural optimization, focussing on the shape of the cut at the hanger ends, has been carried out using evolution strategies.*

The oscillation amplitudes have been computed by means of the Newmark-Wilson time-step method, using an appropriate load model, which has been validated by on-site experiments on the selected reference bridge. Corresponding stress-amplitudes are evaluated by multiplying the oscillation amplitudes with a stress concentration factor. This factor has been computed on the basis of a finite element model of the system "hanger–welding–connection plate", applying solid elements, according to the notch stress approach.

The damage estimation takes into account the stochastics of the exciting wind process, as well as the stochastics of the material parameters (fatigue strength) given in terms of Woehler-curves.

The shape optimization results in a substantial increase of the estimated hanger lifetime. The comparison of the lifetimes of the bulk plate and of the welding revealed that, in the optimized structure, the welding, being the most sensitive part in the original structure, shows much more resistance against potential damages than the bulk material.

1 INTRODUCTION

The high-cycle loading caused by vortex-induced across-wind vibrations frequently leads to visible deteriorations in the suspender connection plates of arched steel bridges. The cracks can occur in the weldings, as well as in the bulk material of the plate. An improper shape of the cut at the hanger-ends leads to high stress peaks which favour the crack-initiation. Therefore, a lifetime-oriented shape optimization method has been developed, based on the stochastic time-dependent fatigue history. The suitability of this method has been checked on the arched steel bridge in Münster-Hiltrup, Germany, which was chosen as a reference-system.

2 SHAPE OPTIMIZATION

The optimization method used — a multi-membered evolution strategy with a self-adaptive mutation mechanism — is based on a finite element analysis applying p-type shell elements. The geometry model has been created using non uniform rational B-splines (NURBS). These curves are used to map the element edges, which are introduced in the blending function method. The advantage of p-type elements is that the initial mesh remains unaltered during the optimization. A total number of 15 design parameters defines the NURBS functions through their control-points. The target function is the weighted sum of the maximal equivalent stresses for the two dominant load cases: tension along the hanger axis and bending. As a constraint, the maximal size of the connection plate has been used. The optimization method is described in detail in [1].

As turned out, the shape of the external plate edge has only little influence on the maximal stress value. Therefore, the optimization has been focussed on the cut at the end of the flattened hanger (see figure 2). The optimization process has been carried out on a cluster of 37 Linux computers, by means of a CORBA-based parallelization scheme.

3 DETERMINATION OF THE STRESS CONCENTRATION FACTORS

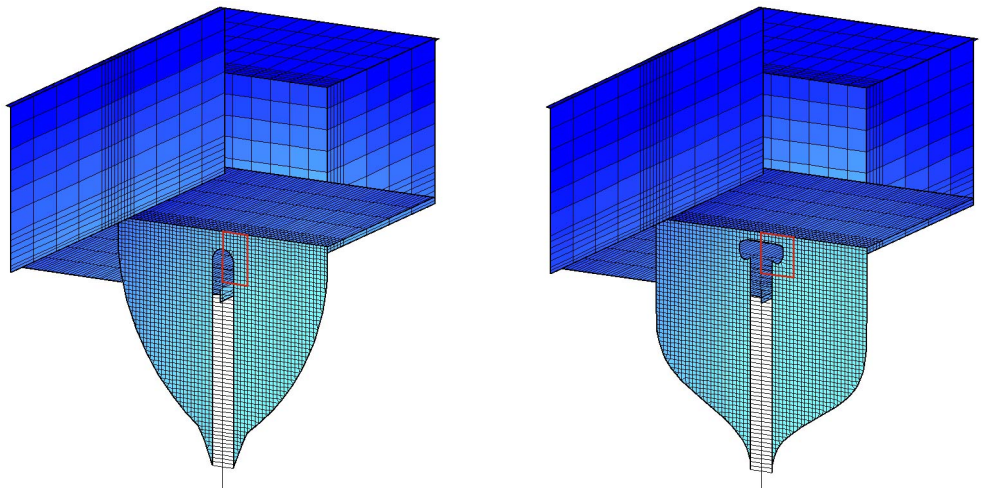

Figure 1: Coarse model of the arch connection plate, consisting of bar- and shell-elements — original geometry (left) and optimized geometry (right)

The stress concentration factors are defined as the maximal stress caused by a rod deflection

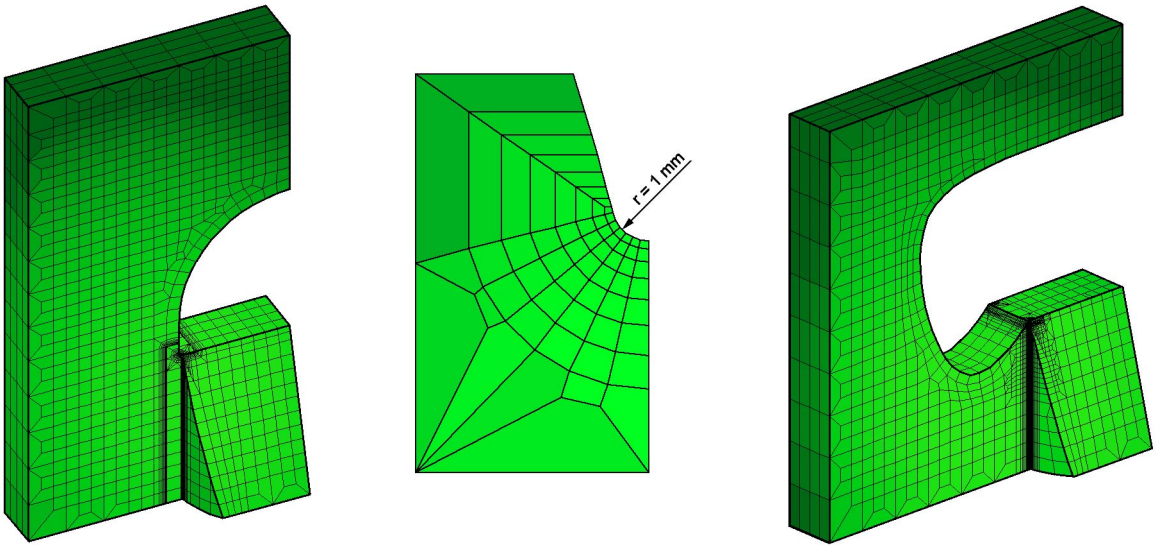

Figure 2: Refined model of the outlined region, consisting of 3D-solid elements — original geometry (left), optimized geometry (right), section through the welding (middle)

of 1 cm. The maximal stresses caused by the oscillation can be calculated by multiplying the displacements of the vibrating tie-rod, measured in cm, with these factors.

As the bulk plate and the welding have different fatigue strengths, the expected lifetime for both components must be determined separately. Consequently, a stress concentration factor for each component is needed. The lifetime analysis of the welding is accomplished according to the notch stress approach (R1MS-concept) formulated in [9]. Thus, the geometry-modelling has to fulfill the percepts formulated therein.

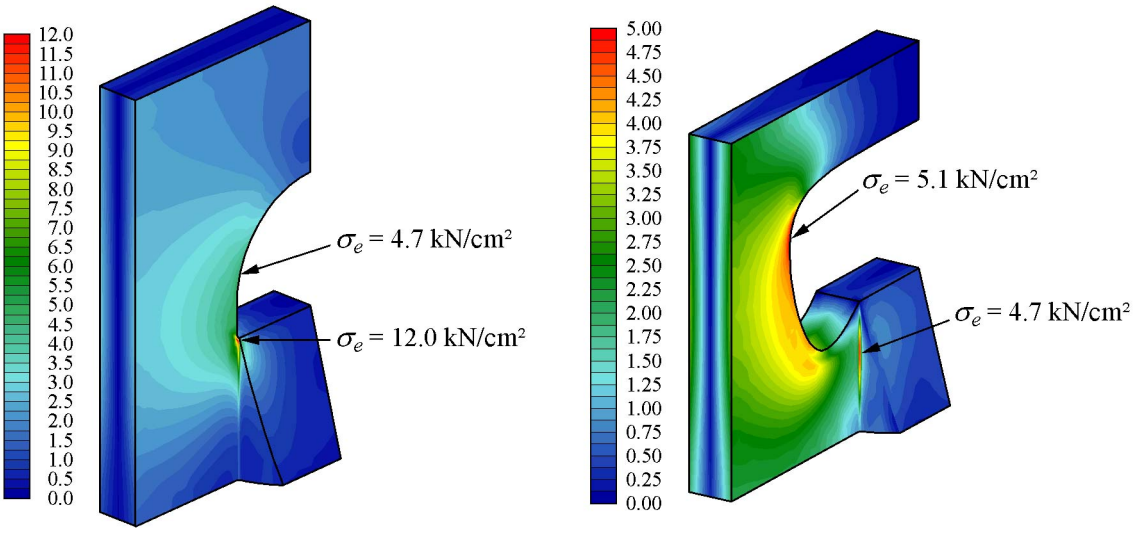

Figure 3: Effective stress caused by a rod deflection of 1 cm for the original geometry (left) and for the optimized geometry (right)

In order to fulfill these prescripts avoiding overwhelming computation times, the concentration factors have been calculated in two steps. First, a realistic, but rather coarse model of the hanger and the connection plates has been created, which consists of bar- and shell-elements (figure 1). At the upper connection plate, also a portion of the arch has been added, including the

separation plate, in order to reproduce the restraint accurately. This was necessary because the relevant load case of this connection plate is bending, which also causes the dominant damage process. Since the lower connection plate is primarily exposed to in-plane strain, its lower edge has been clamped for simplicity. The stifness matrix of the system has been created including the geometric stiffness due to the tension force arising in the hanger because of the bridge self-weight. This finite element model has been used for determining the first eigenshape of the system. This eigenshape, normalised to a maximum deflection of 1 cm, has been used to calculate the displacements and rotations of the nodes in the arch connection plate, on the contours shown in red in figure 1.

Then, a refined finite element model of the critical region (outlined in red) has been created, consisting of 3D-solid elements (figure 2). Herein, the welding notches have been modelled as cylinder barrels with a radius of curvature $r = 1\,\text{mm}$ (see also figure 4), as prescribed in the IIW-guidelines [9]. This model has been subjected to the displacements and rotations of the nodes on the contours, calculated on the coarse model, applied as support displacements and rotations.

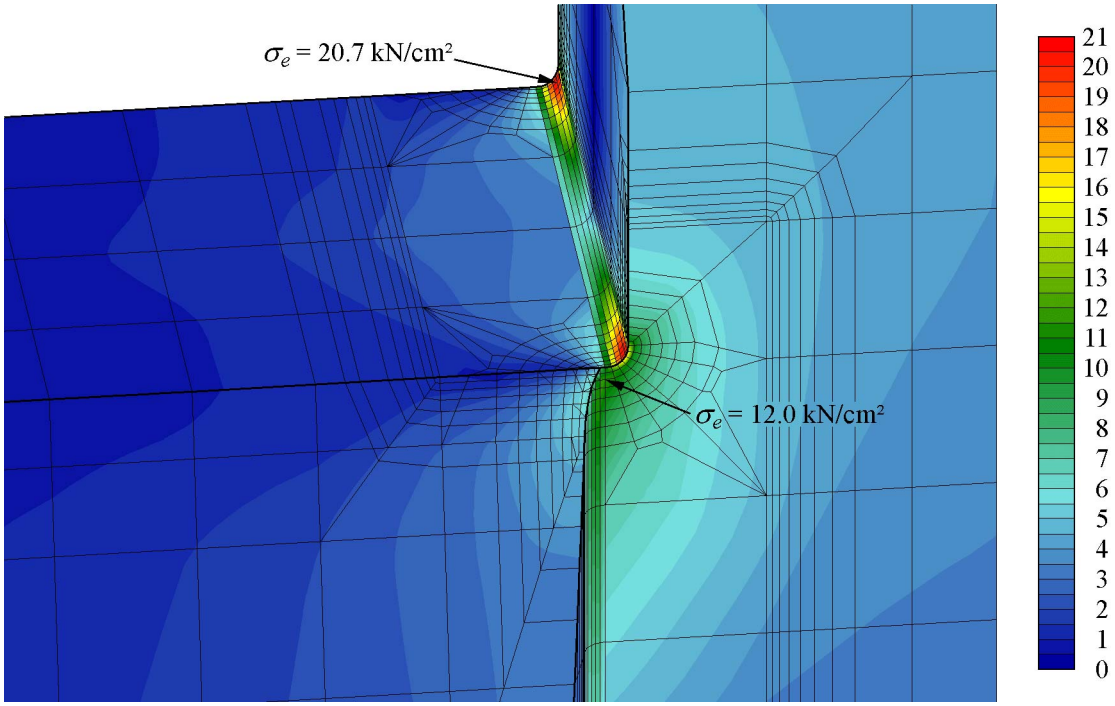

Figure 4: Effective stress in the weldings, caused by a rod deflection of 1 cm, for the original geometry

The effective stresses in the 3D-solid elements are shown in figure 3 and 4. The values refer to the nodes on the structure surface. The arrows mark the position of the maximal stresses in the bulk material and in the welding. The corresponding values are the computed stress concentration factors.

As can be seen, the effective stress in the welding parallel to the plate has been substantially reduced by the optimization — from 12.0 kN/cm^2 to 4.7 kN/cm^2. Moreover, the most critical stress in the original system, which is 20.7 kN/cm^2, has been fully eliminated by removing the re-entrant corner of the cut.

For the original geometry, the maximal stress in the bulk plate cannot be clearly defined, because the stress on the edge of the semi-circular cut increases on approaching the welding.

The value $\sigma_e = 4.7\,\mathrm{kN/cm^2}$, used for the lifetime evaluation, is a local maximum at a height of ca. 32 mm above the re-entrant corner. As can be seen, the stress in the bulk material has been slightly increased by the optimization, reaching the value $\sigma_e = 5.1\,\mathrm{kN/cm^2}$.

4 MEAN WIND VELOCITY DISTRIBUTION FUNCTION

The mean wind velocity plays an essential role in the hanger vibration process because it primarily determines the vortex shedding frequency and thereby the frequency of the excitation force. For the statistical evaluation of the damage process on a large time scale, a velocity distribution function is needed.

The distribution of mean wind velocities $\bar{u}$ over a large period of time — several years — is given by a Weibull function:

$$F_{0W}(\bar{u}) = 1 - e^{-\left(\frac{\bar{u}}{a}\right)^k}, \tag{1}$$

where a and k are the scale and shape parameters. These parameters vary with the wind direction. The values characteristic for Germany have been published by the Deutsche Wetterdienst in [2], where 12 values a_i and k_i, corresponding to 12 sectors of $30°$, are given.

The on-site measurements revealed that the across-wind hanger vibrations occur only in the direction parallel to the bridge axis, i. e. they are only caused by the wind component perpendicular to that axis. This component is characterised by the distribution function

$$F_W(\bar{u}) = \sum_{i=1}^{12} p_i \left[1 - e^{-\left(\frac{\bar{u}}{a_i|\sin\alpha_i|}\right)^{k_i}}\right], \tag{2}$$

α_i representing the angle between the bridge axis and the bisector of the i-th wind direction sector, and p_i the relative occurence frequency of wind velocities lying in this sector. Figure 5 shows the probability density, obtained as the derivative of the distribution function.

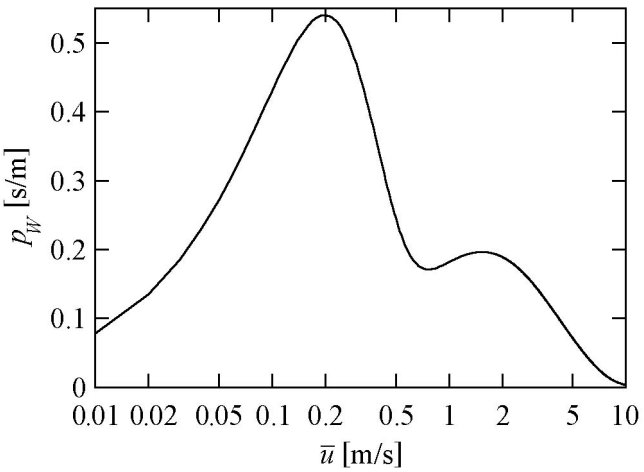

Figure 5: Probability density of the mean wind velocity component perpendicular to the bridge axis

5 CREATION OF THE STOCHASTIC WIND DATA

Besides the mean value, also the fluctuating part of the stochastic wind velocity, which represents the turbulence, has a strong influence on the excitation process. Therefore, the time-history of the wind velocity, used as input for the load model, has to reflect the mean value, the amplitude of scattering, and also the frequency spectrum of the fluctuating wind velocity. This time-history has been created from white noise, which has been transformed to a Gaussian process, and then, to a process exhibiting a Fichtl-McVehil spectral density:

$$\frac{fS_u(f)}{\sigma_u^2} = \frac{a\frac{fL_{ux}}{\bar{u}}}{\left[1 + b\left(\frac{fL_{ux}}{\bar{u}}\right)^r\right]^{\frac{5}{3r}}}. \tag{3}$$

$S_u(f)$, $\bar{u}$ and σ_u^2 are the spectrum at the frequency f, the mean wind velocity and the variance of the fluctuating wind velocity u. L_{ux} denotes the integral length of the turbulent wind, and a, b and r are fit-parameters.

The required spectrum has been obtained by means of the inverse diescrete Fourier-transform. The parameters L_{ux}, a, b and r have been estimated from a fit to the wind data measured on site. Figure 6 presents a comparison of the measured and the fitted spectrum.

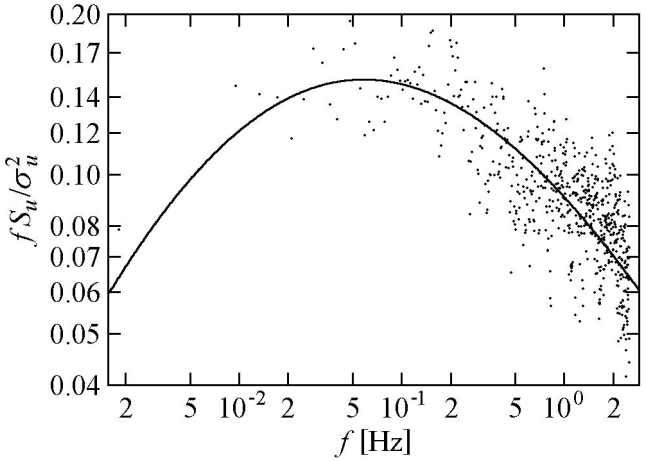

Figure 6: Measured wind velocity spectrum (dots) and fitted Fichtl-McVehil spectrum(solid line)

In the next step, the data have been shifted and scaled, in order to obtain the requierd mean value and variance. For all runs, the same wind turbulence $I_u = \sigma_u/\bar{u}$ has been assumed, i. e. the standard deviation σ_u has been taken proportional to the mean wind velocity. Consequently, the mean value $\bar{u}$ is the only free variable in the definition of the stochastic wind data.

The weak damping (logatithmic damping ratio $\delta \approx 5 \cdot 10^{-4}$) and the large mass of the tie rods lead to extremely slow system answers to changes of the excitation force. This effect can be primarily observed on entering or exiting the *lock-in* range [5]. In order to catch the slow variations of the oscillation amplitude, larger values of ca. 1.5 hours have been chosen for the duration of the wind process.

6 THE WIND LOAD-MODEL

The calculation of the vibration amplitudes requires a load model capable to compute the time-dependent across-wind excitation force from the time-history of the wind velocity. This

excitation force is — alike the wind velocity — a stochastic process. Its frequency varies within an interval around the Strouhal-frequency. The width of this interval increases with the wind turbulence. As the tie rods begin to vibrate, the vortex shedding tends to synchronise itself to the rod motion, giving rise to the *lock-in* effect. This effect, which occures for wind velocities within a critical range, leads to large, resonant oscillations, which play a crucial role in the deterioration process. It also makes the excitation process to become non-stationary, because the nature of the accros-wind force changes on entering or exiting the *lock-in* regime.

Several models have been proposed for predicting the amplitude of the across-wind vibrations [10], [11], [8]. The comparison with experimental data, however, revealed that none of these models predict the amplitudes correctly. Therefore, an adequate wind load model has been developed [5], whose parameters have been trimmed in such a way that the model's predictions show a good agreement with the experiment. The measurements have been carried out on the arched steel bridge in Münster-Hiltrup, Germany, used as a reference-system.

The time-dependent lift force is obtained as

$$F(t) = \frac{\rho}{2} K D C_l L_c \int_0^t u^n(\tau)\, e^{\alpha(t,\tau)} \cos\varphi(t,\tau)\, \mathrm{d}\tau, \tag{4}$$

where ρ is the density of air, D the rod-diameter, C_l the lift coefficient, $u(\tau)$ the fluctuating wind velocity obtained as input, and L_c is the correlation length. K and n are fit-parameters. The arguments of the exponential and of the cosine function are defined as:

$$\alpha(t,\tau) = \int_t^\tau \xi(x)\, \mathrm{d}x, \quad \varphi(t,\tau) = \int_t^\tau \omega(x)\, \mathrm{d}x + \varphi_0(t),$$

$$\xi(x) = \sqrt{\ln 4}\, I_u \omega(x), \quad \omega(x) = \frac{2\pi S}{D}\, u(x),$$

where I_u is the wind-turbulence, ω the fluctuating Strouhal angular frequency and S the Strouhal number. The *lock-in* effect is described by the pamater φ_0, which is set in phase with the rod motion in the *lock-in* regime and to 0 outside of this regime.

Based on this excitation force, the time-dependent deflections have been computed by means of the Newmark-Wilson time-step method. Because of the large number of required runs (wind processes), a simplified finite-element model of the system "hanger–connection plates" has been used, which has been built of bar-elements.

7 PARTIAL DAMAGE EVALUATION

The damage evaluation has been carried out on the tie rod exhibiting the largest vibrations, see [6]. The time-histories of the maximal effective stress in the bulk plate and in the welding have been calculated separately, by multiplying the computed deflections with the corresponding stress concentration factors.

The mean wind velocity $\bar{u}$ has a dominant influence on the stress amplitude, as expected. As has turned out, also the applied initial vibration amplitude A_0 plays an essential role in determining the stress time-history. This is a consequence of the *lock-in* effect, because the width of the critical wind velocity range depends on the vibration amplitude. To catch the influence of both parameters, stress time-histories have been computed for 22 mean wind velocity values $1.0\,\mathrm{m/s} \le \bar{u} \le 10.0\,\mathrm{m/s}$, applying 11 different initial amplitudes $0 \le A_0 \le 1\,\mathrm{cm}$ for each $\bar{u}$. Since the damage considerably varies between stochastic realizations calculated for the same

parameter-pair $(\bar{u}, A_0)$ — i. e. realizations differing only in the particular white noise sample used — 100 processes have been created for each parameter-pair, in order to obtain a suitable statistical distribution. Consequently, a total number of 24200 wind processes, each of the duration $\Delta t \approx 1.5$ hours, have been analysed.

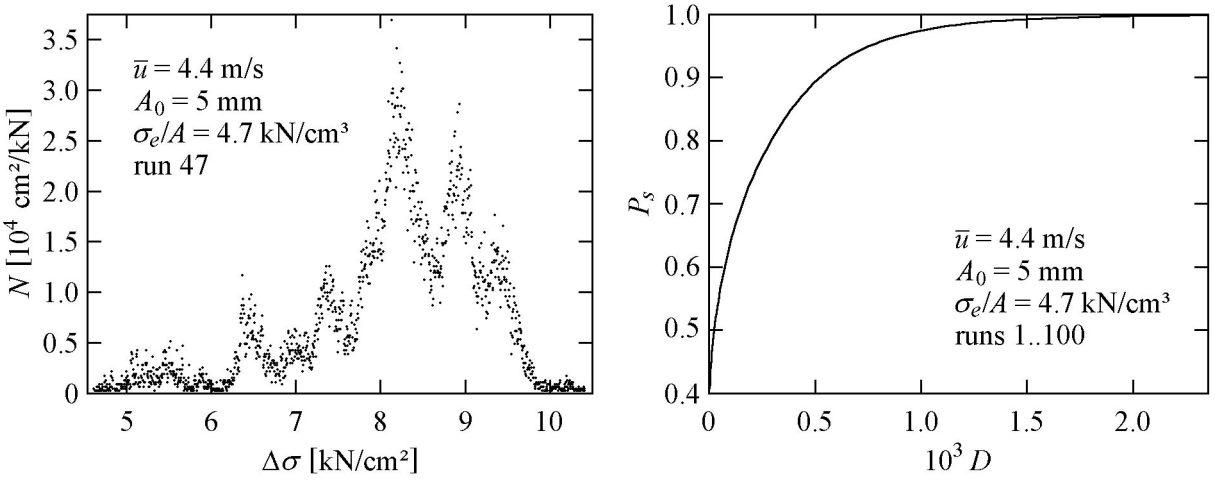

Figure 7: Left: histogram of cycles obtained by the rainflow method, right: corresponding probability function of the partial damage

From the time histories of the effective stresses, the histograms of cycles have been build, using the Clormann-Seeger rainflow counting method [3]. The histogram for a certain run — the occurrence density of cycles plotted vs. the double stress amplitude — is shown in the left panel of figure 7.

For the calculation of the partial damage, the Palmgren-Miner accumulation rule with the modification proposed by Haibach [7] has been used. This rule has been applied to stochastically defined Woehler-curves, which have been generated on the basis of the curves specified in service strength standards. For the weldings, the Woehler-curve given in the IIW-guidelines [9] for geometries modelled according to the R1MS notch stress concept — fatigue class 225 — has been used. The bulk steel plate has been analysed based on the Eurocode 3 Woehler-curve for the fatigue class 160.

The fatigue strength of steel, $\Delta\sigma_D$, exhibits a log-normal distribution. Its value corresponding to a survival probability $P_s = 97.7\,\%$, as well as the slope of the Woehler-curve, $m = 3$, is clearly defined in the standards. However, the standard deviation, which is also needed for the definition of the stochastic curves, is specified in neither standard. Therefore, the value $S_{\log \Delta\sigma_D} = 0.07$, given in the Background informations to Eurocode 3 [4] has been chosen.

The damage accumulated in the bulk plate and in the welding over a large period of time — e. g. one year — can only be evaluated by coupling the stochastics of the loading (histograms of cycles) with the stochastics of the resistance (Woehler-curves). For this purpose, 999 Woehler-curves have been generated, representing equidistant survival probabilities between 0.001 and 0.999, separately for the welding and for the bulk material. For each parameter-pair $(\bar{u}, A_0)$ and a sharp Woehler-curve (e. g. for $P_s = 0.977$), a discrete distribution function of the partial damages, consisting of 100 data, is obtained. These data correspond to the 100 statistically equivalent wind processes, and their distribution reflects the stochastics of the loading. This can be coupled with the stochastics of the resistance by replacing each datum by a set of 999 data

coming from the same wind process, but calculated using the 999 Woehler-curves representing equidistant survival probability values. The data obtained by this procedure yield the distribution function of the partial damage for a parameter-pair $(\bar{u}, A_0)$, reflecting both the stochastics of the loading and of the material properties. A graphical illustration of the probability function, obtained by this method, is presented in the right panel of figure 7.

8 INITIAL AMPLITUDE DISTRIBUTION FUNCTION

For the evaluation of the damage accumulated over the lifetime of the structure, a distribution function of the initial amplitudes A_0 is needed as well. Therefor, a self-consistent, iterative method has been developed. First, the distribution function $F(\bar{u}_i, A_{0j}, A)$ of the amplitude A has been computed from the amplitude time history $A(t)$, for each parameter-pair $(\bar{u}_i, A_{0j})$ ($i = 1..22$, $j = 1..11$). This function has been used to calculate the probabilities of values lying in the vecinity of the applyed initial amplitudes A_{0k}:

$$P(\bar{u}_i, A_{0j}, A_{0k}) = F\left(\bar{u}_i, A_{0j}, \frac{A_{0k} + A_{0\,k+1}}{2}\right) - F\left(\bar{u}_i, A_{0j}, \frac{A_{0k} + A_{0\,k-1}}{2}\right), \quad k = 1..11.$$

The probabilities P_W of wind velocities lying in the vecinity of the applied mean wind velocities $\bar{u}_i$ have been derived from the Weibull distribution function $F_W(\bar{u})$, according to

$$P_W(\bar{u}_i) = F_W\left(\frac{\bar{u}_i + \bar{u}_{i+1}}{2}\right) - F_W\left(\frac{\bar{u}_i + \bar{u}_{i-1}}{2}\right).$$

Then, the probabilities of the 11 applyed initial amplitudes have been initialised to

$$P_A^0(A_{0j}) = \frac{1}{11}, \quad j = 1..11,$$

corresponding to a uniform distribution.

In the nth iteration step, the new amplitude probabilities P_A^{n+1} have been computed from the actual ones (P_A^n) and from the probabilities P_W:

$$P_A^{n+1}(A_{0k}) = \sum_{i=1}^{22} \sum_{j=1}^{11} P_W(\bar{u}_i)\, P_A^n(A_{0j})\, P(\bar{u}_i, A_{0j}, A_{0k}), \quad k = 1..11. \tag{5}$$

The iteration has been finished when no change within the limit of the numerical error ($2 \cdot 10^{-7}$) between two consecutive values of $P_A(A_{0k})$ could be observed:

$$P_A^{n+1}(A_{0k}) = P_A^n(A_{0k}), \quad k = 1..11. \tag{6}$$

Figure 8 presents the probability density obtained as the derivative of the self-consistent initial amplitude probability function. The probability density is a decreasing function of the amplitude, excepting an interval near 8 mm, where a local maximum occurs. This maximum can be probably attributed to the *lock-in* effect, since vibration amplitudes about 8 mm can be often observed in the *lock-in* regime. Initial oscillation amplitudes larger than 11 mm occur with an extremely low probability, since the probability density rapidly drops at amplitudes above 10 mm.

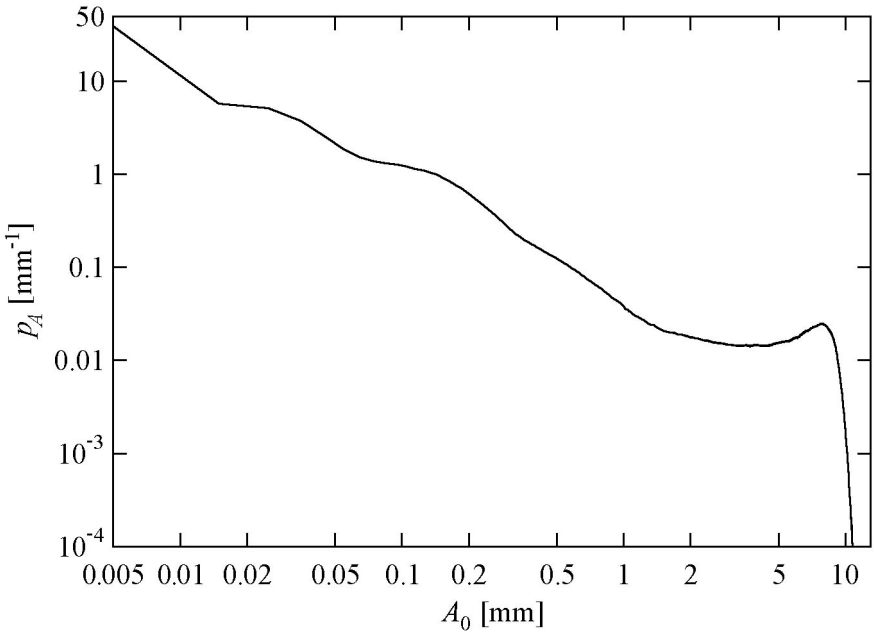

Figure 8: Self-consistent probability density of the initial amplitudes

9 COMPARISON OF THE LIFETIMES

Coupling the methods presented above, the damage accumulated within one year, D_{y}, can be obtained as a function of the survival probability P_s:

$$D_{\mathrm{y}}(P_s) = C \sum_{i=1}^{22} \sum_{j=1}^{11} P_W(\bar{u}_i) P_A(A_{0j}) D(\bar{u}_i, A_{0j}, P_s). \tag{7}$$

$D(\bar{u}_i, A_{0j}, P_s)$ denotes the partial damage calculated for the parameter-pair $(\bar{u}, A_0)$ at the survival probability level P_s (the inverse of the probability function shown in the right panel of figure 7). The factor $C = 6019$ is the number of wind processes per year.

Figure 9 presents the time dependence of the failure probabilities $P_f = 1 - P_s$, for the bulk plate and for the weldings, in the initial and in the optimized geometry. These probabilities have been computed using stochastically defined Woehler-curves, based on the specifications of the Eurocode 3 standard (bulk material) and of the IIW-guidelines (weldings). The time coordinate is obtained as $t = 1/D_{\mathrm{y}}$. The values σ_e are the concentration factors of the effective stress, used in the lifetime evaluation (compare fig. 3 and 4). The highlighted time values represent the lifetimes corresponding to a failure probability of 2.3 %, i. e. to the 97.7 % fractile specified in the Eurocode 3 and in the IIW-guidelines.

The lifetime of the bulk plate has been apparently slightly reduced by the optimization, from 2.4 to 1.5 years. However, as has been pointed out in section 3, the stress concentration factor for the original geometry cannot be clearly defined, thus it can be stated that the lifetime of the bulk plate has not been considerably altered by the optimization.

On the other hand, the lifetime of the welding has been enormously increased, from 0.025 to more than 1000 years. This is primaliry due to the elimination of the re-entrant corner of the cut, which is the most critical region of the original structure. But the lifetime has been also largely increased compared to the value of 0.14 years, characterising the welding parallel to the plate. In the light of this enormous increase, the optimization, focussed on the welding, turned out to be very efficient.

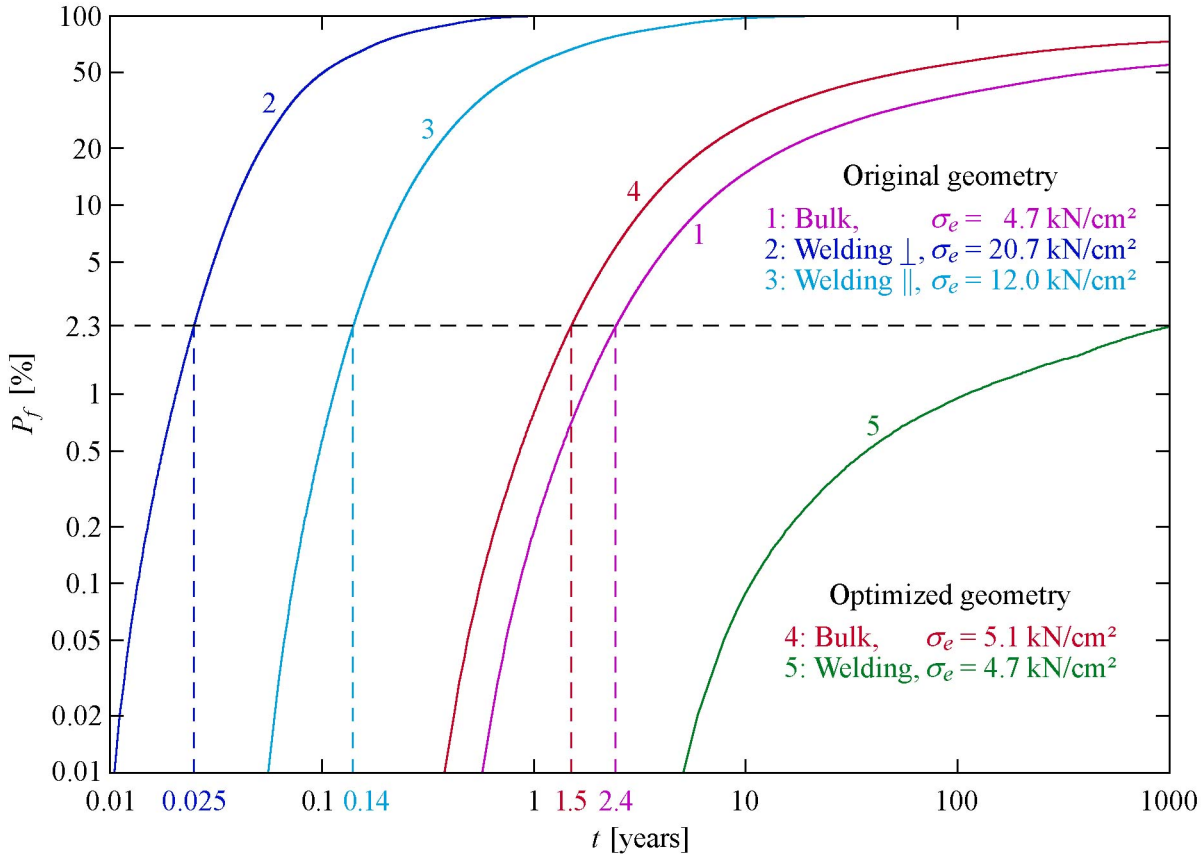

Figure 9: Failure probabilities as a function of time, computed using stochastically defined Woehler-curves

A comparison of the lifetimes in the optimized structure reveals that the welding, by far the most critical part of the original system, is less critical with respect to fatigue damages than the bulk plate.

It should be mentioned, that the building contractor recognized the extremely damage sensitive character of the sharp re-entrant corner and re-designed the welding perpendicular to the plate round-off, using a radius of curvature of about 5 mm. It is supposed that this leads to a substantial increase of the lifetime. Nevertheless, damages in one of the hanger plates have been observed. Currently, these damages are being eliminated.

10 CONCLUSIONS AND OUTLOOK

A method has been developed for estimating the lifetime of the welded hanger connection plates of arched steel bridges subjected to wind load. The suggested method adequately couples the stochastics of the wind load with the probabilistic character of the material properties. Furthermore, a shape optimization procedure has been evolved and tested. The overall lifetime of the connection could substantially be enhanced, from only 0.025 to 1.5 years. The lifetime of the optimized structure is governed by the bulk plate, not by the welding.

Further work will follow up to incorporate the notch-stress approach also in the optimization procedure, aiming at the further encrease of the lifetime of the structural system by balancing the lifetime of the welding with that of the bulk plate. Also, an analysis of the engineered geometry is planned, in order to check the estimated lifetimes against the real-world values.

ACKNOWLEDGEMENTS

We thank R. Höffer and J. Sahlmen *(Aerodynamics Institute of the Ruhr-University Bochum)* for useful discussions. Thanks are also due to the Deutsche Forschungsgemeinschaft which funds the research-work through the SFB 398.

REFERENCES

[1] M. Baitsch and D. Hartmann, Towards Lifetime Optimization of Hanger Connection Plates for Steel Arch Bridges. *Third MIT Conference on Computational Fluid and Solid Mechanics*, Elsevier Science, Cambridge, 2005.

[2] H. Christoffer and M. Ulbricht-Eissing, *Die bodennahen Windverhältnisse in der Bundesrepublik Deutschland.* Berichte des Deutschen Wetterdienstes 147. Selbstverlag des Deutschen Wetterdienstes, 1989.

[3] H. U. Clormann and T. Seeger, Rainflow-HCM. Ein Zählverfahren für Betriebsfestigkeitsnachweise auf werkstoffmechanischer Grundlage. *Stahlbau*, **55**, 3: 65–71, 1986.

[4] Eurocode 3, Part 1. *Background informations on Fatigue design rules. Statistical Evaluation.* Chapter 9 – Document 9.01, 1990.

[5] M. Gálffy, A. Wellmann and D. Hartmann, Modelling of vortex-induced across-wind vibrations on bridge tie rods. *2nd International Conference on Lifetime-Oriented Design Concepts*, Bochum, Germany, 421–429, 2004.

[6] M. Gálffy, A. Wellmann and D. Hartmann, Lifetime-oriented modelling of wind-induced vibrations on vertical bridge tie rods. *Structural Dynamics Eurodyn*, Paris, France, 2213–2218, 2005.

[7] E. Haibach, *Modified linear damage accumulation hypothesis considering the decline of the fatigue limit due to progressive damage*, Laboratorium für Betriebsfestigkeit, Darmstadt, Germany, Techn. Mitt. TM 50/70, 1970.

[8] S. O. Hansen, Vortex-induced vibrations of line-like structures. *CICIND Report*, **15**, No. 1, 1998.

[9] A. Hobbacher, *Recommendations for fatigue design of welded joints and components.* International Institute of Welding (IIW), doc. XIII-1539-96/XV-845-96, 1996.

[10] H. Ruscheweyh, *Dynamische Windwirkungen an Bauwerken.* Bauverlag GmbH Wiesbaden Berlin, 1982.

[11] B. J. Vickery and A. W. Clark, Lift or across-wind response of tapered stacks. *Journal of the Structural Division* (ASCE) **98**, 1–20, 1972.